Polymer Chemistry

ROYAL SOCIETY OF CHEMISTRY

PAPER

View Article Online
View Journal | View Issue

Cite this: *Polym. Chem.*, 2025, **16**, 2372

Two-stepping: sol–gel–gel transitions in a mixed thermoresponsive polymer system†

Mohamad A. Abou-Shamat,[a] Alan Reader,[a] Eleanor Hilton,[b] Niamh Haslett,[a,b] Abhishek Rajbanshi,[a] Najet Mahmoudi,[c] Marcelo Alves da Silva,[d] Jacqueline Stair,[a] Jesus Calvo-Castro[a] and Michael T. Cook*[b]

Received 11th July 2024,
Accepted 7th April 2025

DOI: 10.1039/d4py00771a

rsc.li/polymers

Conventional thermoreversible gels exhibit a sol–gel transition upon modulation of temperature. These systems are typically comprised of block copolymers in which one block exhibits a lower critical solution temperature (LCST), triggering a solvophilic to relatively solvophobic switch of that moiety when heated. The systems, which include poly(ethylene oxide)(PEO)-*b*-poly(propylene oxide)(PPO)-*b*-PEO ("poloxamers") and poly(*N*-isopropylacrylamide) (PNIPAM)-based block copolymers, thus exhibit a single step in their rheological profile upon heating, switching from a predominantly dissipative response to an elastic one. It has been found that a mixed tertiary system of PNIPAM–PEO–PNIPAM and poloxamer 407 displays an unconventional sol–gel–gel transition. The rheological behaviours of this system have been studied to demonstrate the rheological profiles of the sol, "Gel I" and "Gel II" phases, as well as the reversibility of the gelation. A mechanism is proposed for this process, learning from small-angle neutron-scattering experiments in dilute and concentrated regimes.

1. Introduction

Polymers which transition from a solvophilic to a relatively solvophobic state upon heating are said to exhibit a "lower critical solution temperature" (LCST).[1] Using block copolymer solutions, macromolecular design can lead to systems where the LCST system leads to the formation of an elastic mesophase upon warming.[2,3] These polymer solutions are called thermoreversible gels.[4] These materials have wide-ranging applications,[5–7] including use as actuators,[8] pharmaceutical materials,[9] and inks.[10] The mechanisms which drive thermoreversible gel formation in LCST systems typically rely on a hierarchical process where a block copolymer is partially desolvated at the LCST-exhibiting block which triggers self-assembly into nanoscopic aggregates which in turn form a gel network.[4] The pathways that gelation follows depend on the architecture of the constituent polymers.[11,12] ABA copolymers with LCST-exhibiting "B" blocks and hydrophilic "A" blocks can switch from unassociated polymer unimers to core–shell aggregates when warmed above the LCST, which under certain conditions can lead to colloidal jamming or the formation of liquid crystalline phases.[4,13] For example, poloxamer 407 (P407), a poly(ethylene oxide)$(PEO)_{101}$-*b*-poly(propylene oxide)$(PPO)_{65}$-*b*-PEO_{101} polymer, undergoes sol–gel transition in the concentration range of *ca.* 15–35% when heated, transitioning from a liquid phase to a face-centred cubic mesophase.[14]

While the field of thermoreversible gels is quite mature, understanding the behaviour of mixed thermoresponsive systems is not. Poloxamer 407 has been studied to a great extent with polymers that do not exhibit LCST transitions, as well as in binary mixtures with other grades of poloxamers.[15] Constantinou *et al.*[16] have observed synergism in poloxamer 407 mixtures with a poly(oligoethylene glycol methacrylate)-*b*-poly(butyl methacrylate)-*b*-poly(diethylene glycol methyl ether methacrylate) (OEGMA300–BuMA–DEGMA) additive, reporting linear increases in gel strength with incorporation of this second polymer, suggesting that synergy arises from intermicellar association of poloxamer 407 aggregates through bridging with OEGMA300–BuMA–DEGMA. Onoda *et al.* demonstrated that ABC copolymers can be mixed to tune gelation temperatures, based on mixing of micellar aggregates.[17] Block copolymers may also be designed such that there is stereocomplexation between blocks which drives gelation, in a temperature-sensitive manner.[18] It is also known that

[a]*School of Life and Medical Sciences, University of Hertfordshire, Hatfield, AL10 9AB, UK*
[b]*UCL School of Pharmacy, University College London, London, WC1N 1AX, UK. E-mail: michael.t.cook@ucl.ac.uk*
[c]*ISIS Neutron and Muon Source, Rutherford Appleton Laboratory, Harwell Science and Innovation Campus, Didcot, OX11 0QX, UK*
[d]*Institute of Pharmaceutical Science, King's College London, Franklin-Wilkins Building, 150 Stamford Street, London SE1 9NH, UK*
† Electronic supplementary information (ESI) available. See DOI: https://doi.org/10.1039/d4py00771a

mixtures of poloxamer grades allow tuning of gelation temperatures.[19] However, compared to the large literature base on thermoreversible gels,[11,12,20] the current understanding of behaviours of mixed systems and mechanisms driving responsive behaviours is poor.

The ability to access distinct rheological regimes with external triggers has enormous possibilities in fields such as pharmaceuticals, printing, and cosmetics. For example, printing has several different rheological requirements, such as the ability to flow during extrusion without dripping and retain the structure post print.[21] During the printing stage, excessive viscoelasticity can lead to "die swell" effects at the extruder tip, leading to poor spatial control. Immediately post extrusion, however, elasticity is associated with improved print fidelity.[22] The ability to switch between rheological characteristics could therefore be beneficial in developing optimal ink formulations.

This study investigates the effect of an ABA copolymer additive to poloxamer 407 in tertiary mixtures with water. Poly(*N*-isopropyl acrylamide)-*b*-poly(ethylene glycol)-*b*-poly(*N*-isopropyl acrylamide) (PNIPAM–PEG–PNIPAM) was incorporated into thermoreversible poloxamer 407 gels to investigate synergies in these mixtures. PNIPAM–PEG–PNIPAM has been shown in the literature to exhibit reversable thermogelling behaviour in aqueous solution[23] and it is hypothesised that co-micellisation with P407 could be achieved, while exploring the broader questions around emergent behaviours in mixed thermoresponsive gel systems.

2. Results and discussion

PNIPAM–PEG–PNIPAM was prepared by atom-transfer radical polymerisation from a 5 kg mol^{-1} M_n PEG with the PNIPAM chain length targeting an M_n of 10 kg mol^{-1}. The resultant mean degree of polymerisation (DP) of the PNIPAM blocks was found to be 108 from ^{1}H nuclear magnetic resonance (NMR) spectroscopy, with a PEG DP of 97, and the M_n determined by gel permeation chromatography (GPC) was 33.8 kg mol^{-1}, relative to poly(methyl methacrylate) standards in a narrow calibration (Fig. S3†). The dispersity ($Đ$) of the polymer was determined to be 1.8 by gel-permeation chromatography. The resultant copolymer was subsequently denoted N10E5. The full characterisation is described in the ESI.†

Mixtures of N10E5 (10 wt%) and P407 (30 wt%) exhibit an unusual sol–gel–gel behaviour upon heating (Fig. 1i). The con-

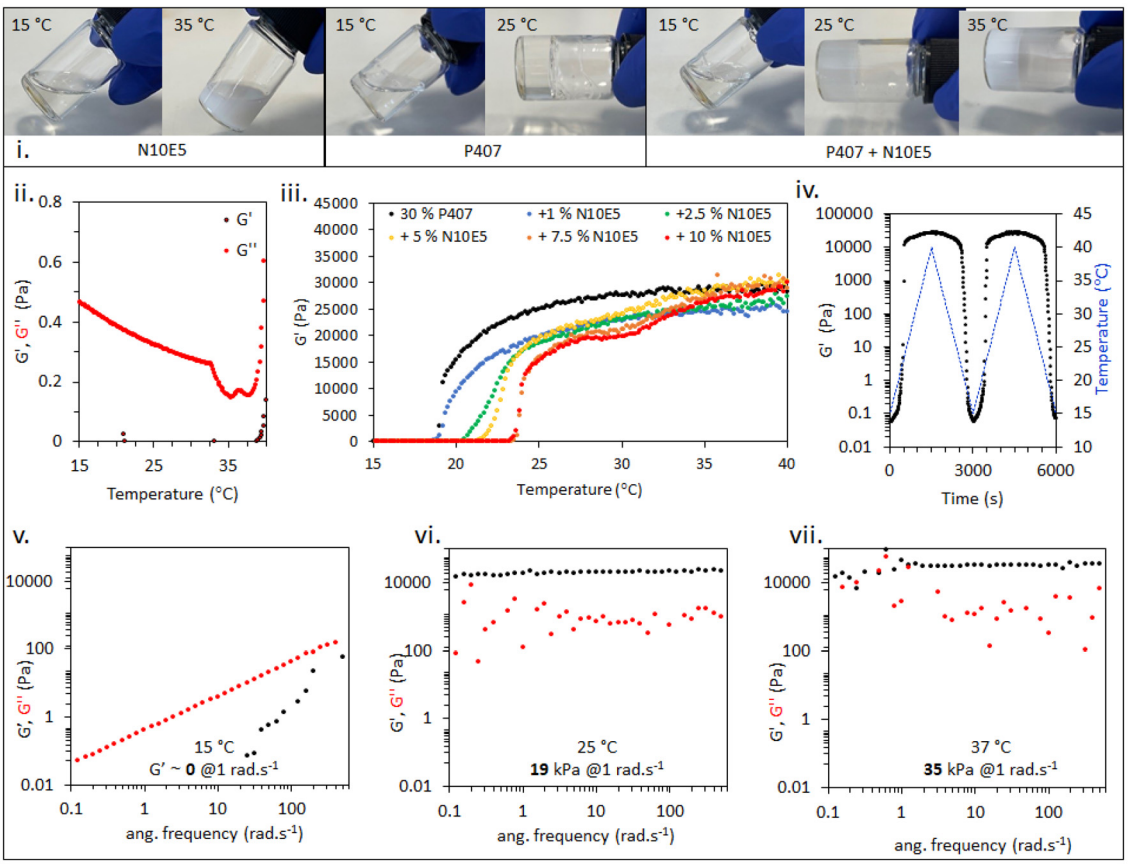

Fig. 1 Macroscopic appearance of N10E5 (10 wt%), P407 (30 wt%), and P407 (30 wt%) + N10E5 (10 wt%) solutions with temperature variation (inset) (i). Temperature-ramp rheograms of N10E5 (7.5 wt%) (ii) as well as P407 and P407 + N10E5 with concentration inset (iii). Reversibility of the gel formed by P407 (30 wt%) + N10E5 (7.5 wt%) probed by small-amplitude oscillatory rheology with a double up–down temperature ramp (iv). Oscillatory frequency sweeps of P407 (30 wt%) + N10E5 (7.5 wt%) at 1 Pa and temperatures of 15 (v), 25 (vi), and 37 °C (vii). Note: object iii is shown with G'' and error from triplicate measurements in Fig. S4 (ESI†). Noise in G'' in these measurements is a result of a very small phase angle (Fig. S5†).

stituent elements at the respective concentrations display either a cloud point temperature without gelation (N10E5)[23] or a single sol–gel transition (P407)[24] whereas the mixture P407 + N10E5 exhibit a transparent low viscosity liquid phase at 15 °C, a translucent gel phase at 25 °C, and a turbid gel phase at 35 °C. The polymer solutions were investigated by small-amplitude oscillatory rheology, setting an oscillatory stress within the linear viscoelastic region and a frequency of 6.283 rad s^{-1}, with variation in temperature to probe modulations in viscoelasticity in the range of 15–40 °C. N10E5 alone gave a weak temperature-dependence of its rheology (Fig. 1ii), with an upward trend of both storage (G') and loss (G'') moduli at temperatures exceeding *ca.* 35 °C albeit with very low absolute values (<0.6 Pa). For mixed systems, the P407 concentration was set at 30% w/v for all formulations, which in a binary mixture with water gave a sol–gel transition temperature (T_{gel}) of 18 °C, defined as the point where G′ exceeds the absolute value of G''. A PNIPAM–PEG–PNIPAM additive, N10E5, was included at 1, 2.5, 5, 7.5, and 10% w/v. The preparations led to an elevation in the T_{gel} as the concentration of N10E5 was increased (Fig. 1iii), pushing this transition from *ca.* 18 to 23 °C. Furthermore, the two gel phases could clearly be observed on the rheogram at higher N10E5 concentrations, giving an upturn in G' at both 23 and 31 °C in the mixtures with ≥7.5 wt% N10E5 added (Fig. 1iii). The reversibility of the transition was also confirmed by a temperature ramp protocol by two heating runs from 25 to 40 °C (Fig. 1iv). No variation in thermal response was observed in these cycles suggesting that the liquid-to-gel transition is fully reversible.

Further rheological analysis of the P407 + N10E5 mixtures was conducted by frequency sweep to probe the nature of the phases present at 15, 25, and 37 °C. G'' was higher than G' at 15 °C throughout the investigated frequency range. Thus, the energy imposed by shear was more dissipated than stored throughout the measured frequencies *i.e.*, the system was behaving as a liquid. At higher temperatures (25, 30 and 37 °C), the formulation's viscoelastic behaviour was altered, with an increase in the absolute values of G' and G'' and transition to a predominantly elastic phase ($G' > G''$). The plateau of the G' values indicates that the formulation acquires permanent elasticity throughout the studied frequencies, giving frequency independence, *i.e.* a gel material. The absolute values of G' at 25 and 37 °C were 19 and 35 kPa, respectively (at 1 rad s^{-1}), indicating an increase in the stored energy in the system at the higher temperature. This supports the formation of a stronger network at 37 °C relative to the 1st gel phase at 25 °C. These phases are hereon referred to as Gel I (25–30 °C) and Gel II (35–40 °C).

The structural nature of the mixed N10E5 + P407 system (Fig. 2i) was investigated by small-angle neutron scattering (SANS), initially considering the behaviour of the constituent macromolecules. N10E5 solutions were investigated by SANS at 7.5 wt% (Fig. 2ii, Tables S2–S5†). SANS scattering data at lower temperature, 25 °C, were fitted with a polydisperse Gaussian coil (PGC) form factor which is related to the system behaving as a mixture of dispersed polymer chains in a theta solvent. In addition, at this temperature a power-law form factor was added to the model to fit the lower q region, which may be related to the contribution from the clustering of the polymer chains in solution.[25,26] With an increase of temperature to 37 and 40 °C, the SANS data could not be fitted with only the PGC form factor, and they were best fit with a combination of a cylinder form factor with 17 and 15 nm radii, respectively, and a PGC to account for the scattering at high q. Additionally, with the increase of the temperature the SANS data were better fitted with a flexible-cylinder form factor with a radius of 13 nm, in concordance with previous work on these systems.[23] This rod-like shape was obtained due to the relatively short PEG segment in the polymer chain, which is unable to facilitate the required curvature for spherical micelles.[23] These cylinders are of indeterminate length, with the end-to-end correlation outside the size range (> *ca.* 100 nm) of the SANS experiments.

The concentrated P407 systems, P407 at 30% and in mixture with N10E5 at 30/7.5 wt%, respectively, were then evaluated by SANS. The data for the concentrated P407 formulation were best fit in the mid and high q ranges with the face-centred cubic (FCC) paracrystal form factor at all temperatures, in line with prior reports of this structure in P407 gels.[27,28] The addition of N10E5 did not affect the formation of this FCC phase in the Gel I phase at 25 °C, allowing the features at $3 \times 10^{-2} < q < 2 \times 10^{-1}$ $Å^{-1}$ to be fit to the FCC paracrystal model at all temperatures. An additional feature became apparent at 37 °C in the Gel II phase and above, centred at 2.3×10^{-2} $Å^{-1}$, corresponding to a correlation distance (d) of 27 nm (using the relation $d = 2\pi/q$). It has been observed that for P407 samples where diblock impurities are present,[29] free chains, in our case N10E5, can occupy the interstitial space in between micelles in the liquid crystal phase creating, due to the depletion effect, a repulsion potential and generating repulsion between the micelles and the free chains promoting higher space between the micelles as indicated by the peak centred at 2.3×10^{-2} $Å^{-1}$. Additionally, increased intensity in the low q region was observed at these temperatures of the Gel II phase and above. Analysis of the low q region below 1×10^{-2} $Å^{-1}$ showed that the reduction in $I(q)$ could be fit with a power law exponent of 2.83 for the P407 system at all temperatures. In the mixed system, the exponent was 3.09 at 25 °C and increased to 3.89 at 37 °C and above. This indicates the formation of a weakly segregated 3D network in the P407 gel. The mixed system contains aggregates with a rough interface at 25 °C, which reduced in roughness upon heating to 37 °C and above.

To better understand the structure of the mixed system, SANS data were collected for N10E5/P407 at 0.75/3.0 (Fig. 2v) and 1.5/3.0 wt% (Fig. 2vi), respectively. At a P407 concentration of 3.0 wt%, Bragg peaks are not observed and $P(q) \times S(q)$ can be properly evaluated. At a lower N10E5 concentration (0.75 wt%), only one spherical object (*ca.* 70 Å) is observed above the T_{gel} and it is attributed to P407 micellar aggregates (Fig. 2v). These micelles show little sensitivity to temperature expect for P407 micelles. At the higher N10E5 concentration

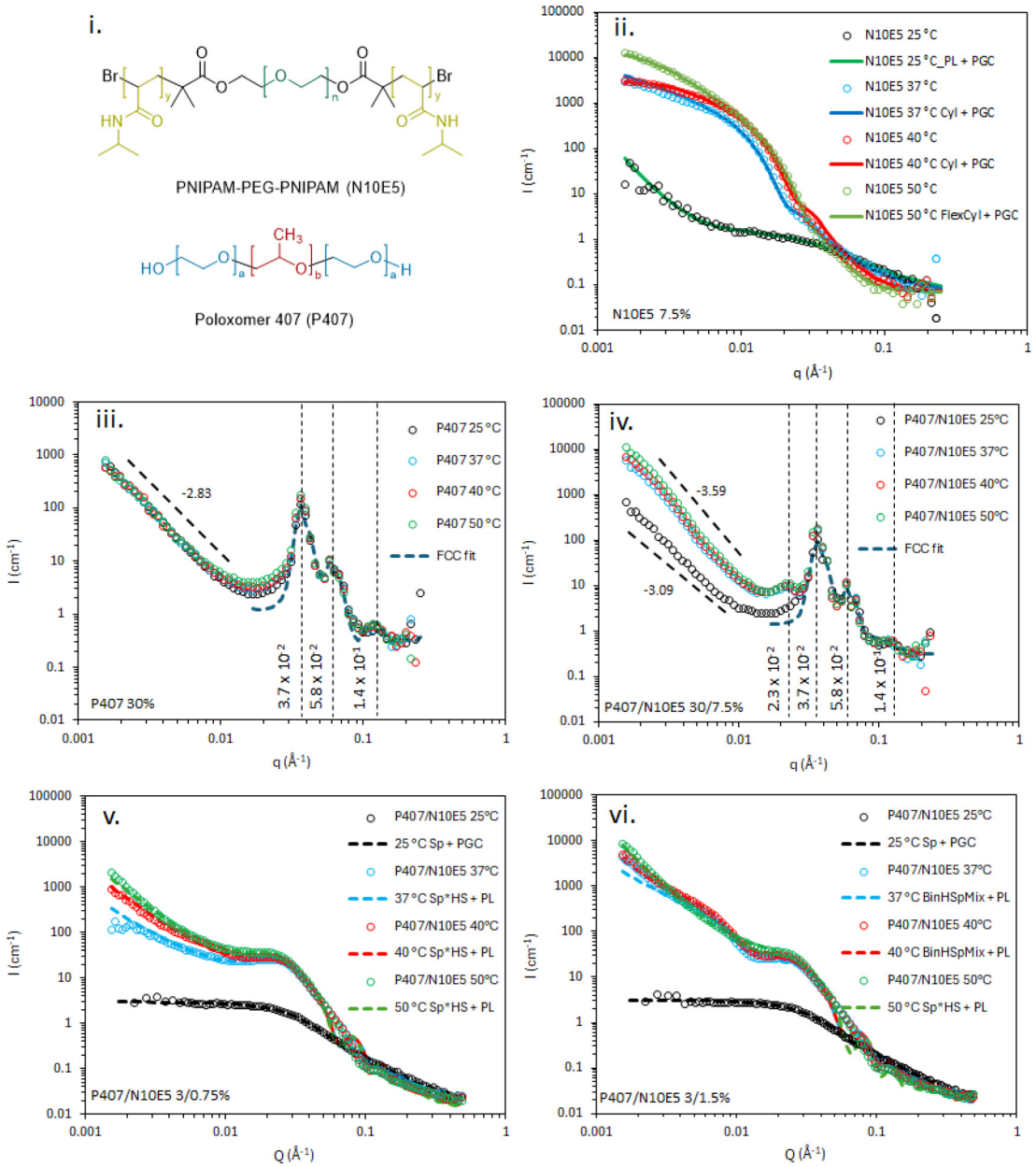

Fig. 2 (i) Chemical structure of N10E5 and P407. (ii) SANS profiles(open symbols) and fits (solid lines) of N10E5 (7.5 wt%) in D_2O at 25, 37, 40 and 50 °C. (iii) SANS of P407 (30 wt%) at 25–50 °C with overlaid dashes highlighting peak positions. Fit to the FCC paracrystal model in mid-to-high q included as a blue dashed line. (iv) SANS of P407 (30 wt%) + N10E5 (7.5 wt%) at 25–50 °C with overlaid dashes highlighting peak positions. (v) SANS data N10E5 0.75 wt% P407 3.0 wt% and (vi) N10E5 1.5 wt% P407 3.0 wt% copolymers as a function of temperature. The abbreviations refer to the form and structure factors used: PL, power law; Sp, sphere; HSp, hard sphere; PGC, polymeric gaussian coil;Cyl: cylinder, and FlexCyl: flexible cylinder. BinHSpMix, binary mixture of spheres + hard sphere, respectively.

(1.5 wt%) (Fig. 2vi), the same spherical object (P407 micelles, *ca.* 70 Å) is observed above the T_{gel}. A second larger spherical object (*ca.* 370 Å) is observed at 37 and 40 °C, but not at 50 °C (Fig. 2vi), and this can be due to the object either being lost or growing beyond the detectable range (> *ca.* 100 nm). For both concentrations a power law component is required to describe the upturn at a lower q, and the upturn indicates the presence of larger structures lying beyond the SANS experiment window, which is attributed to a larger network.

Several considerations are drawn about the mixed P407 + N10E5 system to propose a mechanism for gel formation (Fig. 3). From SANS analysis of the dilute regime, at the lowest concentration (0.75 wt%/3.0 wt% N10E5/P407), only one spherical object is observed above the T_{gel}, and it is considered to be micelles of P407, with a known spherical micellar structure with a PPO core and a PEO corona.[24,30] For 1.55 wt%/3.0 wt% N10E5/P407, a second larger spherical object is observed at 37 and 40 °C, and this object is suggested to occur

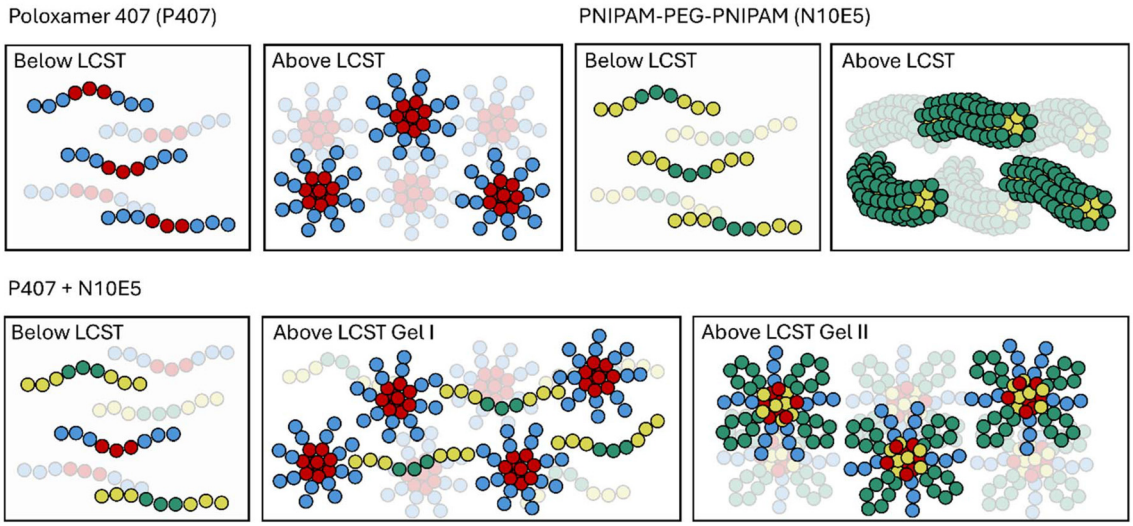

Fig. 3 Proposed gelation mechanism for P407, N10E5, and the P407 + N10E5 composite gel. For P407, blue circles represent PEO and red circles represent the PPO blocks. For N10E5, NIPAM is shown as yellow circles and PEG as green circles.

from the interaction of the N10E5 polymer chains with the corona, considering that PEO is known to cluster in solution.[31] At 40 °C the PNIPAM blocks of N10E5 have begun to desolvate due to the LCST phenomenon, and the NIPAM block of N10E5 would then move from the water phase to the P407 micelle corona, while the PEG block remains in solution. This can lead to N10E5 chains bridging P407 micelles causing their clustering and leading to the formation of this new population of aggregates in addition to a fraction of the P407 particles. At 50 °C the SANS signal shows only the P407 micellar contribution. Thus, it is believed that further NIPAM desolvation moves the NIPAM block deeper in the micelle core, pushing the aggregates to larger sizes beyond the SANS experimental window and generating turbid gels, where the cluster are large enough to scatter in the visible light. In this mixed system, while the curvature of pure N10E5 is limited by the length of the PEG block,[23,32] it is proposed that interdigitation with the poloxamer allows the system to attain a thermodynamically favoured spherical form, albeit with a larger hydrodynamic diameter. This process is diagrammatically shown in Fig. 3, where N10E5 forms "loops" akin to a flower-like micelle; however, it is also likely that the N10E5 chains can also "dangle" as seen in telechelic systems.[33]

In the concentrated regime, SANS confirms that the system formed an FCC structure akin to native P407 at 25 °C, at which point the system is in the Gel I phase. In this case, it is considered that the *ca.* 70 Å micelles observed by SANS can pack into the FCC structure to form a gel. The presence of N10E5 in the system causes some impediment to the cubic gel structure, giving a lower absolute value of G' in the Gel I phase than the corresponding P407 solution (Fig. 1iii). At 50 °C, in the Gel II phase, the N10E5 is able to co-aggregate with the P407 and this impediment to gel formation is removed; however, the larger size of these aggregate gives rise to scattering in the visible range. The rheological response of the Gel II phase has increased the elasticity due to the removal of these impediments to micelle packing.

3. Conclusions

The tertiary N10E5, P407, and water system exhibits a 2-step sol–gel–gel transition upon heating. The basis for this process is proposed to follow a mechanism where P407 alone undergoes micellisation at 23 °C, causing the formation of a liquid crystalline "Gel I" phase. At *ca.* 30 °C the PNIPAM component of N10E5 begins to desolvate, causing interpenetration of N10E5 with the PPO core of P407 micelles and the formation of a mixed micellar system which underpins the Gel II phase. The ability to access more than two rheological phases offers a platform for complex material requirements. For example, in 3D printing, mixing of the encapsulant and ink is favoured in the liquid phase. During extrusion, a viscous material is useful to ensure fidelity of the print and reduce potential nozzle dripping; however, viscous preparations necessitate greater extrusion pressures, which are costly, increase wear, and may damage encapsulants which undergo shear degradation. In post-printing it is preferred that the material retains its structure, aided by increased elasticity. Thus, the blend described herein would allow effective mixing in the sol phase, extrusion in the Gel I phase, and rigidity for shape retention in the Gel II phase. While there are numerous reports of binary water : polymer systems to obtain thermoreversible gels, there is great potential for the expansion of tertiary mixtures with two temperature-responsive gel-formers incorporated. Furthermore, investigating architectural effects of the triblock PNIPAM-*b*-PEG-*b*-PNIPAM system could yield further materials of interest where the block ratio is known to impact self-assembly.

Data availability

The data supporting this article have been included as part of the ESI.† Any additional supporting data are available on request from the authors.

Conflicts of interest

There are no conflicts to declare.

Acknowledgements

The EPSRC (EP/T00813X/1) and Leverhulme Trust (RPG-2023-124) are acknowledged for funding. The STFC ISIS facility is thanked for awarding access to the SANS2D beamline for neutron scattering experiments (**https://doi.org/10.5286/ISIS.E.RB2220037**). This work benefited from the use of the SasView software, originally developed under NSF award DMR-0520547. SasView contains code developed with funding from the European Union's Horizon 2020 research and innovation program under the SINE2020 project, grant agreement no. 654000.

References

1 M. Taylor, P. Tomlins and T. Sahota, *Gels*, 2017, **3**, 4.
2 A. P. Constantinou and T. K. Georgiou, *Eur. Polym. J.*, 2016, **78**, 366–375.
3 A. P. Constantinou and T. K. Georgiou, *Polym. Chem.*, 2016, **7**, 2045–2056.
4 M. T. Cook, P. Haddow, S. B. Kirton and W. J. McAuley, *Adv. Funct. Mater.*, 2020, **8**, 2008123.
5 M. A. Ward and T. K. Georgiou, *Polymers*, 2011, **3**, 1215–1242.
6 B. Jeong, S. W. Kim and Y. H. Bae, *Adv. Drug Delivery Rev.*, 2012, **64**, 154–162.
7 I. Salah, M. Abou-Shamat and M. T. Cook, *J. Appl. Polym. Sci.*, 2019, **136**, 46915.
8 C. Maslen, A. Gholamipour-Shirazi, M. D. Butler, J. Kropacek, I. Rehor and T. Montenegro-Johnson, *Macromol. Rapid Commun.*, 2023, **44**, 19–21.
9 P. Haddow, W. J. McAuley, S. B. Kirton and M. T. Cook, *Mater. Adv.*, 2020, **1**, 371–386.
10 H. Cho, U. Jammalamadaka, K. Tappa, C. Egbulefu, J. Prior, R. Tang and S. Achilefu, *Mol. Pharm.*, 2019, **16**, 552–560.
11 M. A. Ward and T. K. Georgiou, *J. Polym. Sci., Part A: Polym. Chem.*, 2013, **51**, 2850–2859.
12 M. A. Ward and T. K. Georgiou, *Soft Matter*, 2012, **8**, 2737–2745.
13 M. A. Abou-Shamat, J. Calvo-Castro, J. L. Stair and M. T. Cook, *Macromol. Chem. Phys.*, 2019, **220**, 1900173.
14 C. Wu, T. Liu and B. Chu, *J. Non-Cryst. Solids*, 1998, **235–237**, 605–611.
15 M. A. Abou-Shamat, J. Calvo-Castro, J. L. Stair and M. T. Cook, *Macromol. Chem. Phys.*, 2019, **220**, 1900173.
16 A. P. Constantinou, N. Provatakis, Q. Li and T. K. Georgiou, *Gels*, 2021, **7**, 116.
17 M. Onoda, T. Ueki, R. Tamate, A. M. Akimoto, C. C. Hall, T. P. Lodge and R. Yoshida, *ACS Macro Lett.*, 2018, **7**, 950–955.
18 H. Mao, P. Pan, G. Shan and Y. Bao, *J. Phys. Chem. B*, 2015, **119**, 6471–6480.
19 K. Al Khateb, E. K. Ozhmukhametova, M. N. Mussin, S. K. Seilkhanov, T. K. Rakhypbekov, W. M. Lau and V. V. Khutoryanskiy, *Int. J. Pharm.*, 2016, **502**, 70–79.
20 M. A. Ward and T. K. Georgiou, *Polym. Chem.*, 2013, **4**, 1893–1902.
21 R. V. Barrulas and M. C. Corvo, *Gels*, 2023, **9**, 986.
22 H. Herrada-Manchón, M. A. Fernández and E. Aguilar, *Gels*, 2023, **9**, 517.
23 M. A. da Silva, P. Haddow, S. B. Kirton, W. J. McAuley, L. Porcar, C. A. Dreiss and M. T. Cook, *Adv. Funct. Mater.*, 2022, **32**, 2109010.
24 G. Wanka, H. Hoffmann and W. Ulbricht, *Macromolecules*, 1994, **27**, 4145–4159.
25 M. Shibayama, *Polym. J.*, 2011, **43**, 18–34.
26 B. Hammouda, *Polymer*, 2009, **50**, 5293–5297.
27 F. Sakuma, K. Higashi, K. Ueda, T. Morita, D. Iohara, F. Hirayama and K. Moribe, *Langmuir*, 2024, **40**, 15610–15620.
28 R. K. Prud'homme, G. Wu and D. K. Schneider, *Langmuir*, 1996, **12**, 4651–4659.
29 K. Mortensen, W. Batsberg and S. Hvid, *Macromolecules*, 2008, **41**, 1720–1727.
30 G. Wanka, H. Hoffmann and W. Ulbricht, *Colloid Polym. Sci.*, 1990, **268**, 101–117.
31 B. Hammouda, D. L. Ho and S. Kline, *Macromolecules*, 2004, **37**, 6932–6937.
32 A. Blanazs, S. P. Armes and A. J. Ryan, *Macromol. Rapid Commun.*, 2009, **30**, 267–277.
33 A. N. Semenov, J. F. Joanny and A. R. Khokhlov, *Macromolecules*, 1995, **28**, 1066–1075.